

# Geophysical Research Letters

RESEARCH LETTER  
10.1029/2018GL081274

**Key Points:**

In rainy years, recharge from the watershed rapidly altered wetland soil temperatures, affecting sedge abundance and methane emissions. When wetland soils were warmed by spring rainfall, growing-season methane emissions increased by ~30%. By advecting thermal energy into soil, precipitation regulates the near-term global warming potential of thawing permafrost landscapes.

**Supporting Information :**  
• Supporting Information SI

**Correspondence to:**  
R.B.Neumann,  
rbneum@uw.edu

**Citation :**  
Neumann, R.B., Moorberg, C.J., Lundquist, J.D., Turner, J.C., Waldrop, M.P., McFarland, J.W., et al. (2019). Warming effects of spring rainfall increase methane emissions from thawing permafrost. *Geophysical Research Letters*, 46. <https://doi.org/10.1029/2018GL081274>

Received 13NOV 2018  
Accepted 26 DEC 2018  
Accepted article online 3JAN 2019

## Warming Effects of Spring Rainfall Increase Methane Emissions From Thawing Permafrost

Rebecca B. Neumann<sup>1</sup>, Colby J. Moorberg<sup>1</sup>, Jessica D. Lundquist<sup>1</sup>, Jesse C. Turner<sup>1</sup>, Mark P. Waldrop<sup>3</sup>, Jack W. McFarland<sup>3</sup>, Eugenie S. Euskirchen<sup>4</sup>, Colin W. Edgar<sup>4</sup>

and Merritt R. Turetsky<sup>5</sup>

<sup>1</sup>Department of Civil and Environmental Engineering, University of Washington, Seattle, WA, USA, <sup>2</sup>Department of Agronomy, Kansas State University, Manhattan, KS, USA, <sup>3</sup>U.S. Geological Survey, Menlo Park, CA, USA, <sup>4</sup>Institute of Arctic Biology, University of Alaska Fairbanks, Fairbanks, AK, USA, <sup>5</sup>Department of Integrative Biology, University of Guelph, Guelph, Ontario, Canada

**Abstract** Methane emissions regulate the near-term global warming potential of permafrost thaw, particularly where loss of ice-rich permafrost converts forest and tundra into wetlands. Northern latitudes are expected to get warmer and wetter, and while there is consensus that warming will increase thaw and methane emissions, effects of increased precipitation are uncertain. At a thawing wetland complex in Interior Alaska, we found that interactions between rain and deep soil temperatures controlled methane emissions. In rainy years, recharge from the watershed rapidly altered wetland soil temperatures, warming the top ~80 cm of soil in spring and summer and cooling it in autumn. When soils were warmed by spring rainfall, methane emissions increased by ~30%. The warm, deep soils early in the growing season likely supported both microbial and plant processes that enhanced emissions. Our study identifies an important and unconsidered role of rain in governing the radiative forcing of thawing permafrost landscapes.

**Plain Language Summary** Because the world is getting warmer, permanently frozen ground around the arctic, known as permafrost, is thawing. When permafrost thaws, the ground collapses and sinks. Often a wetland forms within the collapsed area. Conversion of permanently frozen landscapes to wetlands changes the exchange of greenhouse gases between the land and atmosphere, which impacts global temperatures. Wetlands release methane into the atmosphere. Methane is a potent greenhouse gas. The ability of methane to warm the Earth is 32 times stronger than that of carbon dioxide over a period of 100 years. In our study, we found that methane release from a thaw wetland in Interior Alaska was greater in rainy years when rain fell in spring. When spring rainwater entered the wetland, it rapidly warmed wetland soils. Rain has roughly the same temperature as the air, and during springtime in northern regions, the air is warmer than the ground. The microbial and plant processes that generate methane increase with temperature. Therefore, wetland soils, warmed by spring rainfall, supported more methane production and release. Northern regions are expected to receive more rainfall in the future. By warming soils and increasing methane release, this rainfall could increase near-term global warming associated with permafrost thaw.

### 1. Introduction

When ice-rich permafrost thaws, the ground subsides, creating thermokarst features such as thaw wetlands (Kokelj & Jorgenson, 2013). Permafrost thaw triggers an immediate loss of previously frozen soil organic carbon that is eventually offset (over centuries to millennia) by carbon sequestration in wetland biomass that subsequently forms (Frolking et al., 2006; Jones et al., 2017). However, wetlands also generate methane, and methane emissions can cause these carbon-sequestering systems to have a positive global warming potential over decades to centuries (Frolking et al., 2006; Johansson et al., 2006; Turetsky et al., 2007), the timescale of relevance for climate projections and policy (Saunois et al., 2016).

In boreal regions, warming temperatures have (Poulter et al., 2017) and will continue (Zhang et al., 2017) to increase wetland methane emissions by promoting permafrost thaw and creating new wetland area. Northern latitudes are also expected to receive more rainfall (Bintanja & Andry, 2017; Euskirchen et al., 2016), and few studies have accounted for the ability of rain to alter soil temperature, which is a key control on plant and microbial processes involved with methane production and emissions (Yvon-Durocher et al., 2014).

To a first approximation, rain has the same temperature as air (Byers et al., 1949), and when air and soil temperatures are mismatched, rainwater inputs can rapidly change subsurface soil temperatures through thermal conduction. Previous studies imply that rain is an important transporter of thermal energy into soil in northern latitudes. Thaw depth within permafrost regions appears associated with precipitation amount (Grant et al., 2017; Iijima et al., 2014; Olivas et al., 2011; Quinton et al., 2009), while thermal modeling of northern peatlands, which ignored advective heat transport by rain, was unable to match measured soil temperatures when large precipitation events occurred (Kettridge & Baird, 2008). Most biogeochemical models do not include advective heat transport and thus cannot accurately simulate soil temperatures for a wetter future, undermining prediction of biogeochemical processes. Here we present data clearly demonstrating the power of rain to rapidly alter soil temperatures within a thaw wetland in Interior Alaska and affect methane emissions.

Our site was thawing wetland complex located within a black spruce forest (*Picea mariana* Mill.) underlain by ice-rich permafrost (Euskirchen et al., 2014; Figure 1a). Over 3 years (2014–2016) we used eddy covariance to measure carbon, water, and energy flux in the bog and surrounding permafrost forest and collected meter-scale plant and carbon flux data from the bog (Figure 1e). The data set is unique because we captured an average precipitation year (2015 had 283 mm of rainfall; 30-year normal rainfall for the area is 230–289 mm; NOAA, 2017) and 2 years with abnormally high rainfall (378 mm in 2014 and 345 mm in 2016; Figure 2b). Additionally, the bogs have floating peat mats, which facilitated a consistent water table depth relative to the peat surface all 3 years (Figure S1 in the supporting information). With no notable change in thickness of unsaturated peat, we avoided the confounding effects that a change in water table depth can have on thermal conductivity of soil (Hillel, 2005) and on production and oxidation of methane (Olefeldt et al., 2013; Turetsky et al., 2014).

## 2. Methods

### 2.1. Site Description

The studied wetland complex, in Interior Alaska, 30 km southwest of Fairbanks (64.70°N, -148.3°W), is situated in discontinuous permafrost. It is located within the Bonanza Creek Long Term Ecological Research forest and is part of the Alaska Peatland Experiment. The wetland is classified as a bog because it is recharged only by precipitation and runoff from the surrounding forested peat plateaus (Figure 1a). The ~1-m-thick peat soils in forested plateaus have a low bulk density ( $0.27 \pm 0.16 \text{ g/cm}^3$ ; mean  $\pm$  standard deviation) and high field water content ( $74 \pm 16 \text{ vol.}\%$ ; Manies et al., 2017). The bogs are composed of ~70-cm-thick peat mats (bulk density,  $0.06 \text{ g/cm}^3 \pm 0.03 \text{ g/cm}^3$ ; field water content,  $86 \pm 10 \text{ vol.}\%$ ) that float on top of a ~70-cm-thick watery peat layer (bulk density,  $0.21 \pm 0.20 \text{ g/cm}^3$ ; field water content,  $89 \pm 11 \text{ vol.}\%$ ) that is underlain by mineral soil (Marries et al., 2017; Figure 1a).

Thaw commenced at the site 50 to 400 years ago and is active along bog margins (Euskirchen et al., 2014; Klapstein et al., 2014). When ice-rich permafrost thaws, the land subsides and soils are flooded. Fast-growing aquatic plant species such as sedges and hydrophilic *Sphagnum* mosses colonize the area (Finger et al., 2016). With increasing time following thaw, peat accumulates, and hummock-hollow microtopography develops, enabling woody plants to grow in the drier elevated hummocks while hollows remain saturated throughout the growing season. The centers of bogs represent areas where thaw initiated while the edges of bogs represent areas that recently thawed; bog age increases from edge to center. As such, bog edges include open water transitioning into *Sphagnum riparium* hummocks with vascular plants such as water sedge (*Carex* spp.), bog rosemary (*Andromeda polifolia* L.), cotton grass (*Eriophorum* spp.), and leather leaf (*Chamaedaphne calyculata*), while the older bog centers are dominated by *Sphagnum* spp. hummocks that support woody species such as dwarf and bog birch (*Betula nana* and *Betula glandulosa*) and larch (*Larix laricina*; Finger et al., 2016). Hollows in the bog center support a similar diversity of vascular species as bog edges.

Along the edge-to-center transect, growing-season soil temperatures increase in years with average precipitation (i.e., the center is warmer because it is further from permafrost), while *Carex* density, methane emissions, and total dissolved nitrogen concentrations decrease (Finger et al., 2016; Neumann et al., 2016; Figure 1b).

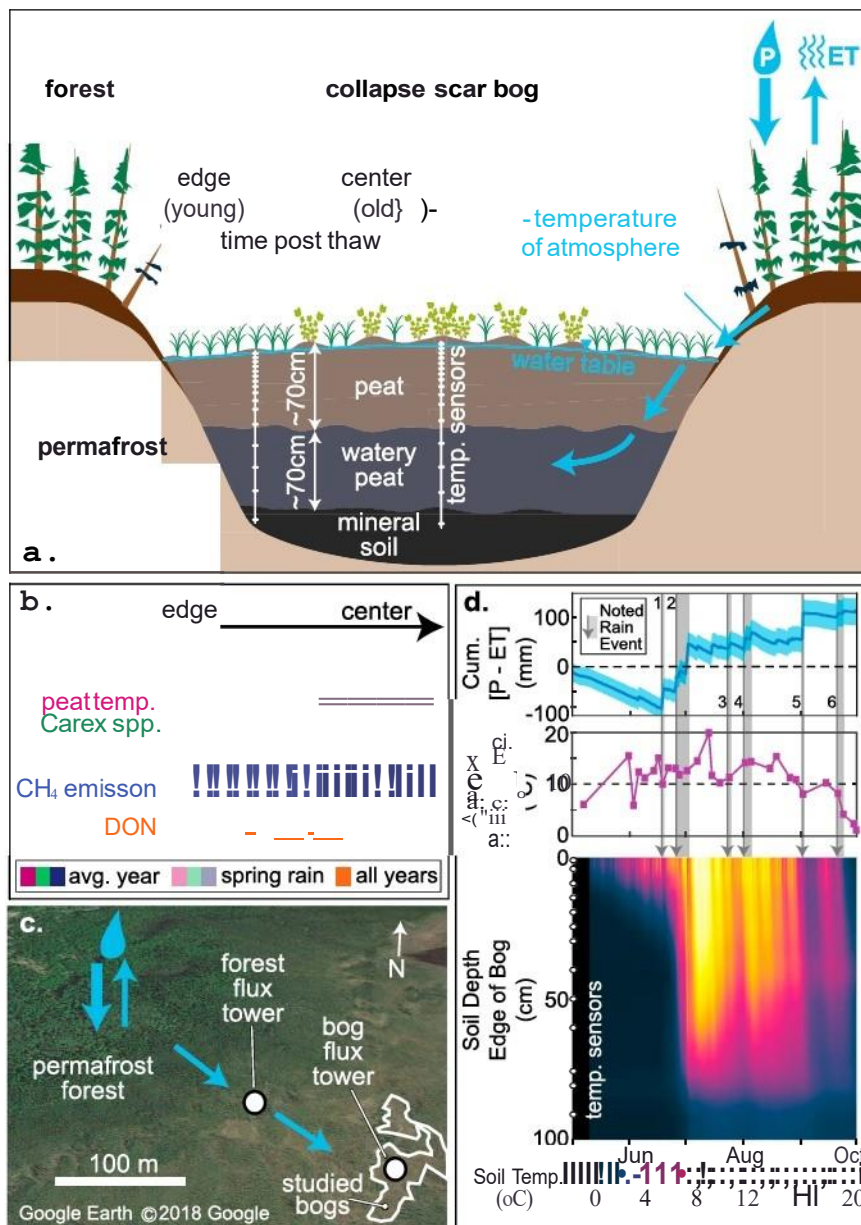


**Figure 1.** Conceptual overview. (a) Collapse scar bog surrounded by forested permafrost plateaus. The bog has ~70-cm-thick peat mat that floats on a watery peat layer underlain by mineral soil. The permafrost is actively thawing at the bog edge while thaw initiated 50 to 400 years ago in the bog center. The younger bog edge includes open water transitioning into *Sphagnum* hummocks. The older bog centers have *Sphagnum* hummocks that support woody species. *Carex* is the dominant vascular species at the bog edge and in hollows of the bog center. Temperature sensors were installed at multiple depths at the edge and center of the bog. When cumulative rainfall exceeds cumulative evaporative water loss in the forest, temperature data indicate water from the surrounding permafrost forest enters at the bog edge where it plunges down vertically and then travels horizontally through the watery peat layer toward the bog center. (b) Conceptual representation of edge-to-center gradients of soil temperature, coverage of *Carex*, methane emissions, and dissolved organic nitrogen (DON) concentrations in the bog for an average year (e.g., 2015; dark colored bands) and a year with spring rainfall (e.g., 2016; light colored bands). DON gradients are not affected by rainfall. Gradients are based on data presented in this manuscript, except for DON concentrations, which are based on data in Finger et al. (2016). (c) Google Earth image of field site showing the permafrost forest that contributes water to the down-gradient bog complex. Location of flux towers installed within the permafrost forest and bog complex are indicated. (d) Data collected from the site during 2014. Top panel, cumulative difference between precipitation (P) and evapotranspiration (ET) for the permafrost forest. Arrows mark rain events, with duration of events highlighted by the gray bars associated with each arrow. Arrow 1 indicates a rain event that did not contribute water to the bog because the cumulative rain amount had not yet offset the cumulative ET demand for the forest. All other arrows mark rain events that did contribute water to the bog. Middle panel, estimated temperature of rain, which was calculated as the volume-weighted temperature of the air when the rain fell. Bottom panel, soil temperature (indicated by color according to the color bar) as a function of time and depth for the bog edge. (Data for the bog center is in Figure S2.) Depths of temperature sensors are marked with white circles along y-axis. Arrows 2 and 4 show events that occurred when rainfall was warmer than soil, resulting in rapid penetration of warmer temperatures into soil. Arrows 3, 5, and 6 indicate rain events that occurred when rainfall was cooler than soil, resulting in rapid penetration of colder temperatures into soil.

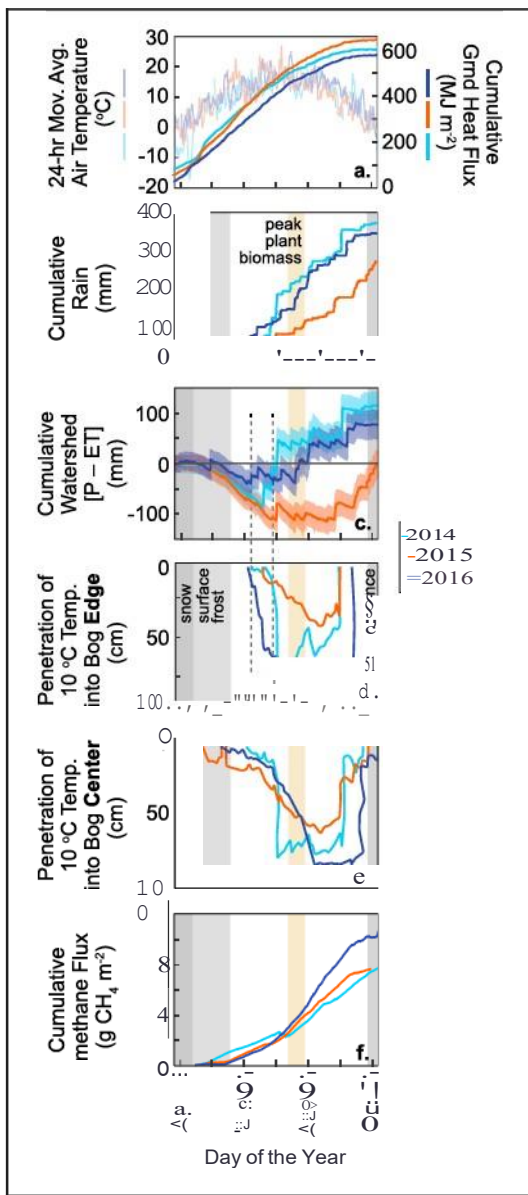


Figure 2. Comparison of data from 2014, 2015, and 2016. (a) Air temperature and cumulative ground heat flux in the bog. (See section SI for heat flux calculation). (b) Cumulative rainfall (mm). An average amount of precipitation occurred in 2015, while 2014 and 2016 were abnormally wet. (c) Cumulative seasonal difference between precipitation (P) and evapotranspiration (ET) in the permafrost forest. Positive values indicate cumulative amount of rainfall exceeded cumulative ET demand. (d) Time versus penetration depth of 10°C at the bog edge. In 2014 and 2016, the two rainy years, soil rapidly warmed to 10°C, aligning with the point in time when cumulative rainfall amount met or exceed the ET water loss of the upland permafrost forest (see dashed lines connecting panels c and d). In 2016, soil at the edge warmed to 10°C 3 weeks earlier than it did in 2014. The sharp midseason shallowing of the 10°C contour in 2014 was a result of rain that fell during a cool day in July (see arrow 3, Figure 1d). (e) Time versus penetration depth of 10°C in the bog center. (f) Cumulative methane flux for the bog complex measured via eddy covariance. Gray bars across panels b-f mark typical persistence of snow cover and presence of seasonal frost in the bog, along with the typical point in the growing season when plants reach peak biomass and senesce.

## 2.2. Soil Temperature Measurement

Soil temperatures were measured following the methods of Cable et al. (2016) using calibrated temperature probes consisting of 16 thermistors (10-K ohm thermistor PIN PS203J2, U.S.Sensor, Orange, CA) embedded in a urethane matrix to form a single 150-cm-long rod. Following calibration, each probe was inserted into the bog. Temperatures were continuously measured to a depth of 150 cm for the 3 years of the study. Measurements were recorded using a Campbell CR1000 data logger (Campbell Scientific, Logan UT). Because of upward sensor drift, measurements from sensors with readings above 0 °C on 1 January of each year were adjusted downward to 0 °C. The adjustment was applied to measurements for the entire year of data. This correction resulted in a temperature step-change on 1 January for the adjusted measurements depths, but a smooth and continuous record for the remainder of the year. Upward sensor drift was detected by looking at temperatures recorded by shallow sensors in early winter when diurnal temperature variation disappeared, indicating the presence of frost. The flatline temperature associated with the onset of frost should be -0 °C. Over the three study years, the flatline temperature got progressively warmer, necessitating the step adjustment.

## 2.3. Flux Tower Measurements

Fluxes of methane, water, and energy were collected with two eddy covariance measurement stations, one placed in the thermokarst bog complex and one in the permafrost forest. At both locations, basic microclimatic data were also collected in conjunction with the eddy covariance data. The eddy covariance and microclimatic measurements are detailed in Euskirchen et al. (2014). Both the processed eddy covariance and microclimatic data were averaged for 30-min periods. Data gaps in eddy covariance data, related to instrument error or malfunction, calm periods (friction velocity,  $u^* < 0.2 \text{ m/s}$ ), or power outages, were filled by calculating the mean diurnal variation, where a missing observation was replaced by the mean for that time period (half hour) based on adjacent days (Falge et al., 2001).

## 2.4. Site-Level Measurements

Site-level methane fluxes were measured approximately weekly from June to September using conventional static chamber techniques (Turetsky et al., 2008). Chambers (area  $0.36 \text{ m}^2$ , height 0.60 m) were constructed from metal sheets that were painted white to reduce chamber temperatures and were placed on metal collars permanently embedded into the peat surface both near the edge and center of the studied bog. Collars were accessed using permanent raised boardwalks. Fans within the flux chamber mixed headspace gas during sampling, which included collection of a 20-ml gas sample into a plastic syringe fitted with a stopcock every 5 min over a 30-min period (total of seven samples per flux). Samples were returned to the lab and analyzed for CH<sub>4</sub> concentrations within a 24-hr period using a Varian 3800 gas chromatograph with an FID detector with a Haysep N column (Varian Analytical Inc., Palo Alto, CA, USA). Flux rates were calculated as the slope of linear regressions of CH<sub>4</sub> concentrations versus time. Fluxes with poor fits ( $r < 0.8$ ) were not included. Methane fluxes were statistically compared using the nonparametric Wilcoxon rank-sum test, which indicates if populations have statistically different distributions. Plant data were collected from

gas flux collars during peak biomass (middle to late July). Each year, percent cover of all vascular and bryophyte species was visually estimated. In 2014, stems of vascular species were counted within five 8-cm by 8-cm subsections of collars and scaled up based on collar area, while in 2015 and 2016, stems were counted within entire collars. In all 3 years, heights of vascular species were measured relative to the bog surface within five 8-cm by 8-cm subsections of collars.

### 3. Results and Discussion

#### 3.1. Amount and Timing of Rainfall Affects Bog Soil Temperatures

Deep soil temperatures were warmer in years with high rainfall relative to the average precipitation year (Figures 2d and 2e). However, cumulative annual net heat flux into the bog determined from a classical energy balance (section S1) was lower in the rainy years (622 and 583 MJ/m<sup>2</sup> in 2014 and 2016, respectively, versus 654 MJ/m<sup>2</sup> in 2015; Figure 2a). Thus, we attribute warmer soil temperatures in 2014 and 2016 to rain and not to radiation.

During the two rainy years, we observed rapid penetration of warmer temperatures into soil down to depths 2:::75 cm during the first rain events that occurred after cumulative evaporative water loss from the upland watershed area had been met or exceeded by cumulative rainfall (arrow 2, Figure 1d; arrows 2 and 9, Figure S2). This situation enabled rainwater to move through the upland watershed, enter and recharge the bog rather than remain in upland soils where it is transpired by plants (Figures 1a and 1e). During early rain events, air temperatures, and thus rainwater temperatures, were 2:::10 °C, while average temperatures within the top 75 cm of bog soil were 5 °C. Thus, rainwater recharge rapidly increased soil temperatures, particularly at the bog edge (arrow 2, Figure 1d; arrows 2 and 9, Figure S2). In the permafrost forest, soil temperatures closely follow air temperatures, generating runoff with similar temperatures to that of rainfall (Figure S3). When cumulative evaporative water loss from the upland watershed area was not met by cumulative rainfall, bog recharge and rapid warming of soil did not occur (arrow 1, Figure 1d; arrows 1 and 7, Figure S2). Rather, slow progressive warming associated with radiative energy input was observed.

The ability of rainwater recharge to alter bog soil temperatures down to deep depths was also demonstrated by rapid soil cooling when rain was colder than soil, predominantly in the fall (arrows 5 and 6, Figure 1d; arrows 5, 6, 8, and 11, Figure S2), and also on a cool day in July 2014 (arrow 3, Figure 1d). During midsummer, when rain and soil temperatures were similar, rainwater recharge did not notably alter soil temperatures but helped maintain and progress warm temperatures to deeper depths (arrow 4, Figure 1d; arrows 4 and 10, Figure S2).

#### 3.2. Post-Rain Recharge Creates Spatial Gradients in Bog Soil Temperature

Multipie studies have found that edges of actively thawing wetlands are hotspots for microbial processing of organic matter, including methane production, and assumed responses were driven by inputs of recently thawed permafrost carbon, which is easily degraded by microbes and often co-occurs with other nutrients (Abbott et al., 2014; Anthony et al., 2016; Finger et al., 2016; Keuper et al., 2012; Klapstein et al., 2014; Neumann et al., 2016; Turetsky et al., 2002). Our data suggest another plausible mechanism. We found that upland water enters the bog edge and then plunges downward and moves laterally toward the bog center (Figure 1a), and thus, temperature responses were stronger at the bog edge than in the center (Figures 2d, 2e, and S2). As such, in rainy years, soils at wetland edges can warm earlier and/or more intensely than wetland centers.

Temperature data from a large rain event in 2014 (arrow 2, Figure 1d) illustrate the bog recharge pattern. During the event, the top 150 cm of soil at the bog edge experienced warming, and temperatures in the top 60 cm converged (Figure S4a). However, in the center, only soil at depths 80 to 135 cm experienced warming (Figure S4a), indicating that warm water from the edge moved laterally to the center through deep soil layers. Similar transitioning of vertical to lateral flow has been reported for peatlands with raised recharge locations and soil layers with different hydraulic conductivities (Reeve et al., 2000; Waddington & Roulet, 1997). The delay in soil-temperature response relative to this and other rain events indicates it takes 5-6 days for water from the upland watershed to enter the bog (Figure S4).

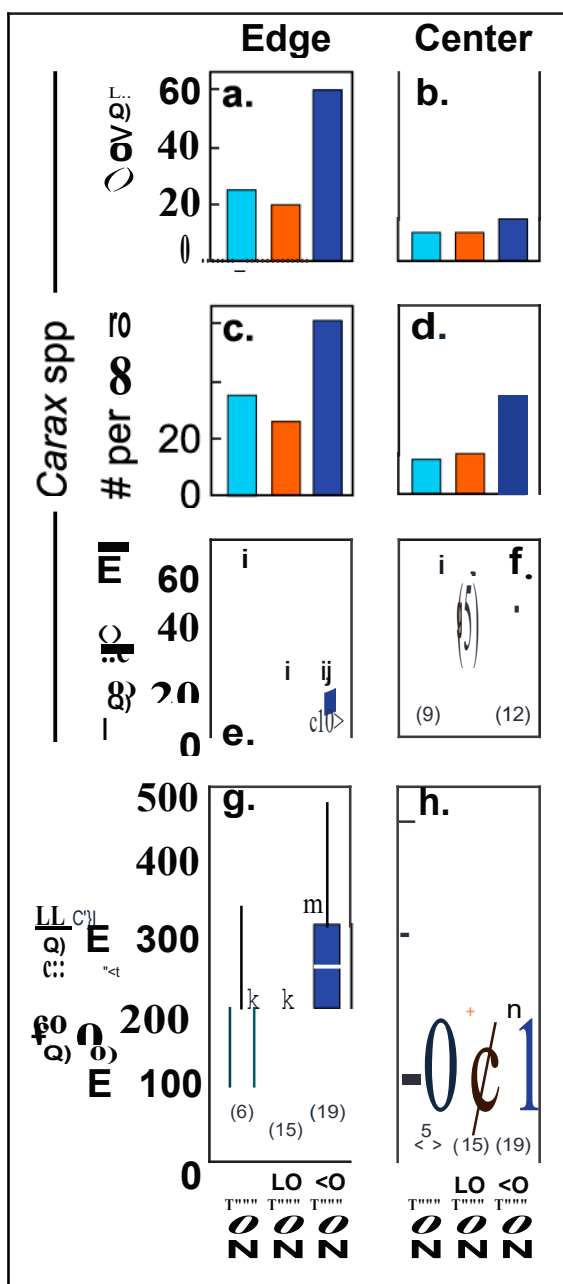


Figure 3. Bog-level data for 2014–2016. (a,b) Percent cover of *Carex* plants in flux collars during peak biomass near the (a) edge and (b) center of the bog. (c,d) Number of *Carex* plants in flux collars during peak biomass near the (c) edge and (d) center of the bog. (e,f) Box and whisker plot of *Carex* height measured during peak biomass in flux collars near the (e) edge and (f) center of the bog. (e,f) Box and whisker plot of growing-season (June to September) methane emissions from flux collars near the (e) edge and (f) center of the bog. In panels (e-h) the central mark on the box marks the median, and the bottom and top edges of the box mark the 25th and 75th percentile, respectively. Whiskers extend to the most extreme data points not considered outliers. Outliers are marked with "+" symbol. Numbers in parentheses below boxes indicate the number of data points in each data set. Letters at top of boxes indicate data sets with statistically different distributions ( $p < 0.05$ ) according to the nonparametric Wilcoxon rank-sum test.

### 3.3. Timing of Rain-Induced Warming Governs Soil Biogeochemical Response

Rain fell earlier in 2016 than in 2014 (Figure 2b), facilitating earlier warming of soil at the bog edge. In 2016, relative to 2014, shallow soil at the bog edge warmed to  $10^{\circ}\text{C}$  approximately 20 days earlier, while soil down to -60-cm depth was fully warmed to  $10^{\circ}\text{C}$  approximately 15 days earlier (Figure 2d). This early warming at the bog edge in 2016 was coincident with increases of between 100% and 200% in number and coverage of *Carex* spp., the dominant sedge species at the site, relative to the two previous years (Figures 3a and 3c). It is well established that methane production and emissions increase with sedge productivity because sedges release carbon into soil that can fuel methane production and contain hollow internal tissues called aerenchyma that facilitate diffusion of methane from soil to atmosphere (Joabsson et al., 1999; King et al., 1998; Olefeldt et al., 2013). As such, in 2016, median methane emissions at the bog edge were  $259 \text{ mg}\cdot\text{m}^{-2}\cdot\text{d}^{-1}$ , 56% and 100% larger than median emissions from the edge in 2014 and 2015, respectively (Figure 3g).

In contrast, later warming of the bog edge in 2014 (Figure 2d) corresponded with smaller increases (between 25% and 35%) in number and coverage of *Carex*, relative to 2015, the average precipitation year (Figures 3a and 3c). Statistically, methane emissions at the bog edge in 2014 and 2015 were indistinguishable (Figure 3g). In the bog center, where soils experienced minimal rain-induced warming (Figure 2e), *Carex* coverage did not markedly change across the 3 years (Figure 3b). *Carex* numbers increased in 2016 (Figure 3d), but plant height decreased (Figure 3f), resulting in no apparent change in coverage. Correspondingly, methane emissions in the bog center were statistically similar all 3 years (Figure 3h).

Studies conducted in northern latitudes indicate that aboveground biomass, height, and cover of sedges increase with warming (Hollister et al., 2005; Shaver et al., 1998; van der Wal & Stien, 2014; Walker et al., 2006). The positive growth response reflects a direct plant physiological effect and/or temperature-induced increase in plant-available nutrients (Chapin, 1983). Microbial processing of soil organic matter and the corresponding generation of plant-available nutrients intensifies with temperature (Alster et al., 2018). Here we infer that rain-induced warming of soil facilitated microbial production of plant-available nutrients across the soil profile. In 2016, when rain warmed soils early in the growing season, microbial generation of these nutrients aligned with the early growth phase during which northern-latitude plants rapidly take up soil nutrients (Chapin et al., 1975). Others working in thawing permafrost landscapes have found that plant productivity increases in response to warmer soil temperatures during the spring rather than during the summer (Helbig et al., 2017). *Carex* are particularly responsive to increased nutrient availability because they have a high nutrient demand (Shaver et al., 1998) and are deeply rooted, enabling access to nutrients in deep soil unavailable to other species (Finger et al., 2016). At our site, dissolved organic nitrogen concentrations are higher at the bog edge than in the center and increase with depth (Finger et al., 2016). Thus, there is a nitrogen pool that can, after microbial processing, support *Carex* growth—particularly at the bog edge where *Carex* abundance and methane emissions increased in 2016 (Figure 3a).

At the landscape scale, eddy covariance measurements indicated that cumulative methane emissions increased by ~30% in 2016 relative to the two previous years (Figure 2f). This increase at the landscape scale can be explained by the increase in methane emissions at the bog edge (Figure 3g) if edge areas cover ~25% of land area, which is reasonable given the flux tower footprint (Figure S5). Thus, a relatively small, biologically active area of the landscape responded to spring rainfall and influenced large-scale carbon exchange, illustrating the importance of biogeochemical "hotspots" and "hot moments" (McClain et al., 2003) within thawing landscapes.

Rainfall is often associated with increased methane emissions, but this connection is attributed to rain increasing the water table and decreasing thickness of unsaturated soil where methane oxidation occurs (Turetsky et al., 2014). At our site, no significant change in thickness of unsaturated peat was observed between the 3 years because the bogs have floating peat mats (Figure S1), reinforcing that rainfall increased methane emissions by warming soil and altering plant and microbial processes rather than by changing water table position.

### 3.4. Biogeochemical Feedbacks to Climate in a Wetter Future

Our study demonstrates that amount and timing of rain regulate soil temperatures within thaw bogs, which affects sedge abundance and methane emissions. Bog edges most recently converted from permafrost are the most sensitive to impacts from rain due to rain recharge patterns (Figure 1a). As boreal regions experience additional permafrost thaw (Jorgenson et al., 2006; Zhang et al., 2017) and projected increases in precipitation, most notably in the amount of early-season rainfall (Bintanja & Selten, 2014; Euskirchen et al., 2016), our data indicate methane emissions can increase and accelerate near-term global warming.

In an effort to contextualize our results, we estimate that if, in a wetter future, early rainfall routinely warms soils in boreal regions and causes methane emissions to double from 10% of wetland area (i.e., a conservative estimate of edge area at our site; Figure S5), it would increase boreal methane emissions by ~4 Tg CH<sub>4</sub> per year (SI section 2). An increase of ~4 Tg CH<sub>4</sub> per year is noteworthy given biogeochemical models that ignored advective transport of thermal energy estimated boreal wetland methane emissions increased at a rate of ~1.2 Tg C per year during the early part of the 21st century (Poulter et al., 2017). These models also project that during the latter part of the 21st century, natural wetland emission will continue to increase at a rate of 0.6 to 2 Tg C per year (Zhang et al., 2017). This growth in wetland methane emission was due to increases in atmospheric temperature and wetland area. The potential perturbation to methane emissions resulting from early-season rainfall is equivalent to between 2.5 and 8 years of emissions growth caused by these two factors, and it could be sustained as permafrost continues to thaw and new bog edges develop.

Capturing and correctly accounting for dynamic biosphere-atmosphere interactions and feedbacks, such as those involved with permafrost thaw, requires modeling. However, most biogeochemical models do not include advective heat transport. Our study points to precipitation as an important transporter of thermal energy into soil, particularly in northern latitudes where air and soil temperatures are often mismatched. Incorporating advective heat transport into models is readily possible (Kurylyk et al., 2014), but it requires improvement of precipitation projections, which are highly uncertain relative to temperature projections (Intergovernmental Panel on Climate Change, 2013). Our study indicates the thermal impact of rain on soil biogeochemistry could be substantial, representing an important knowledge and modeling gap in advancing environmental predictability.

### References

- Abbott, B. W., Larouche, J. R., Jones, J. B., Bowden, W. B., & Balser, A. W. (2014). Elevated dissolved organic carbon biodegradability from thawing and collaing permafrost: Permafrost carbon biodegradability. *Journal of Geophysical Research: Biogeosciences*, 119, 2049-2063. <https://doi.org/10.1002/2014JG002678>
- Alster, C.J., Weller, Z.D., & von Fischer, J.C. (2018). A meta-analysis of temperature sensitivity as a microbial trait. *Global Change Biology*, 24(9), 4211-4224. <https://doi.org/10.1111/gcb.14342>
- Anthony, K. W., Daanen, R., Anthony, P., von Deimling, T.S., Ping, C.-L., Chanton, J.P., & Grosse, G. (2016). Methane emissions proportional to permafrost carbon thawed in Arctic lakes since the 1950s. *Nature Geoscience*, 9(9), 679-682. <https://doi.org/10.1038/ngeo2795>
- Bintanja, R., & Andry, O. (2017). Towards a rain-dominated Arctic. *Nature Climate Change*, 7(4), 263-267. <https://doi.org/10.1038/nclimate3240>
- Bintanja, R., & Sellen, F.M. (2014). Future increases in Arctic precipitation linked to local evaporation and sea-ice retreat. *Nature*, 509(7501), 479-482. <https://doi.org/10.1038/nature13259>

### Acknowledgments

We thank Andrea Wong, Anna Tsai, Mickey Jarvi, and Steve Blazewicz for field assistance; Bill Riley and Qing Zhu for helpful discussions about biogeochemical models; and Jennifer Harden and David McGuire for their participation in the APEX research program. This material is based upon work supported, in part, by the U.S. Department of Energy, Office of Science, Office of Biological and Environmental Research under award number DE-SC0010338 to R. B. N. and the USGS Land Change Science Program. Considerable logistic support was provided by the Bonanza Creek LTER Program, which is jointly funded by the NSF (DEB 1026415) and the USDA Forest Service, Pacific Northwest Research Station (PNWOL- NII 2619320-16). This is contribution No. J9-009-J of the Kansas Agricultural Experiment Station. Any use of trade names is for descriptive purposes only and does not imply endorsement by the U.S. Government. Data used in this publication are available on the Bonanza Creek LTER website ([www.lteruaf.edu/data.cfm](http://www.lteruaf.edu/data.cfm)).

Byers, H.R., Moses, H., & Hamey, P.J. (1949). Measurement of rain temperature. *Journal of Meteorology*, 6(1), 51-55. [https://doi.org/10.1175/1520-0469\(1949\)006<0051:MORT>2.0.CO;2](https://doi.org/10.1175/1520-0469(1949)006<0051:MORT>2.0.CO;2)

Cable, W. L., Romanovsky, V. E., & Jorgenson, M. T. (2016). Scaling-up permafrost thermal measurements in western Alaska using an ecoregion approach. *The Cryosphere*, 10(5), 2517-2532. <https://doi.org/10.5194/tc-10-2517-2016>

Chapin, F.S. M. (1983). Direct and indirect effects of temperature on arctic plants. *Polar Biology*, 2(1), 47-52. <https://doi.org/10.1007/BF00258285>

Chapin, F.S. M., Cleve, K. V., & Tieszen, L. L. (1975). Seasonal nutrient dynamics of tundra vegetation at Barrow, Alaska. *Arctic and Alpine Research*, 7(3), 209. <https://doi.org/10.2307/1549997>

Euskrich, E. S., Bennett, A. P., Breen, A. L., Genet, H., Lindgren, M. A., Kurkowski, T. A., et al. (2016). Consequences of changes in vegetation and snow cover for climate feedbacks in Alaska and Northwest Canada. *Environmental Research Letters*, 11(10), 105003. <https://doi.org/10.1088/1748-9326/11/10/105003>

Euskrich, E. S., Edgar, C. W., Turetsky, M. R., Waldrop, M. P., & Harden, J. W. (2014). Differential response of carbon fluxes to climate in three peatland ecosystems that vary in the presence and stability of permafrost: Carbon fluxes and permafrost thaw. *Journal of Geophysical Research: Biogeosciences*, 119, 1576-1595. <https://doi.org/10.1002/2014JG002683>

Falge, E., Baldosa, D., Olson, R., Anthoni, P., Aubine, M., Bemhofer, C., et al. (2001). Gap filling strategies for defensible annual sums of net ecosystem exchange. *Agricultural and Forest Meteorology*, 107(1), 43-59. [https://doi.org/10.1016/S0168-1923\(00\)00225-2](https://doi.org/10.1016/S0168-1923(00)00225-2)

Finger, R. A., Turetsky, M. R., Kielland, K., Ruess, R. W., Mack, M. C., & Euskrich, E. S. (2016). Effects of permafrost thaw on nitrogen availability and plant-soil interactions in a boreal Alaskan lowland. *Journal of Ecology*, 104(6), 1542-1554. <https://doi.org/10.1111/1365-2745.12639>

Frolking, S., Roulet, N., & Fuglestvedt, J. (2006). How northern peatlands influence the Earth's radiative budget: Sustained methane emission versus sustained carbon sequestration. *Journal of Geophysical Research*, 111, G01008. <https://doi.org/10.1029/2005JG000091>

Grant, R. F., Mekonnen, Z. A., Riley, W. J., Wainwright, H. M., Graham, D., & Tom, M. S. (2017). Mathematical modelling of Arctic polygonal tundra with Ecosys: 1. Microtopography determines how active layer depths respond to changes in temperature and precipitation: Active layer depth in polygonal tundra. *Journal of Geophysical Research: Biogeosciences*, 122, 3161-3173. <https://doi.org/10.1002/2017JG004035>

Helbig, M., Quinton, W. L., & Sonnentag, O. (2017). Warmer spring conditions increase annual methane emissions from a boreal peat landscape with sporadic permafrost. *Environmental Research Letters*, 12(11), 115009. <https://doi.org/10.1088/1748-9326/aa8c85>

Hillel, D. (Ed) (2005). *Encyclopedia of soils in the environment*. Cambridge, MA, USA: Academic Press. Retrieved from <https://www.sciencedirect.com/science/article/pii/S0970123485304/encyclopedia-of-soils-in-the-environment>

Hollister, R. D., Webber, P. J., & Tweedie, C. E. (2005). The response of Alaskan arctic tundra to experimental warming: Differences between short- and long-term responses. *Global Change Biology*, 11(4), 525-536. <https://doi.org/10.1111/j.1365-2486-2005-00926.x>

Iijima, Y., Ohta, T., Kotani, A., Fedorov, A. N., Kodama, Y., & Maximov, T. C. (2014). Sap flow changes in relation to permafrost degradation under increasing precipitation in an eastern Siberian larch forest. *Ecohydrology*, 7(2), 177-187. <https://doi.org/10.1002/eco.1366>

Intergovernmental Panel on Climate Change (2013). *Climate change 2013: The physical science basis Contribution of Working Group I to the Fifth Assessment Report of the Intergovernmental Panel on Climate Change*. (T.F. Stocker, D. Qin, G.-K. Plattner, M. Tignor, S.K. Allen, J. Boschung, et al., Eds.). Cambridge, United Kingdom and New York, NY, USA: Cambridge University Press. Retrieved from <https://www.ipcc.ch/report/ar5/wg1/>

Joabsson, A., Christensen, T. R., & Wallen, B. (1999). Vascular plant controls on methane emissions from northern peatforming wetlands. *Trends in Ecology & Evolution*, 14(10), 385-388. [https://doi.org/10.1016/S0169-5347\(99\)1649-3](https://doi.org/10.1016/S0169-5347(99)1649-3)

Johansson, T., Maimer, N., Crill, P. M., Friberg, T., Akerman, J. H., Mastepanov, M., & Christensen, T. R. (2006). Decadal vegetation changes in a northern peatland, greenhouse gas fluxes and net radiative forcing. *Global Change Biology*, 12(12), 2352-2369. <https://doi.org/10.1111/j.1365-2486.2006.01267.x>

Jones, M. C., Harden, J., O'Donnell, J., Manies, K., Jorgenson, T., Treat, C., & Ewing, S. (2017). Rapid carbon loss and slow recovery following permafrost thaw in boreal peatlands. *Global Change Biology*, 23(3), 1109-1127. <https://doi.org/10.1111/gcb.13403>

Jorgenson, M. T., Shur, Y. L., & Pullman, E. R. (2006). Abrupt increase in permafrost degradation in Arctic Alaska. *Geophysical Research Letters*, 33, L02503. <https://doi.org/10.1029/2005GL024960>

Kettridge, N., & Baird, A. (2008). Modelling soil temperatures in northern peatlands. *European Journal of Soil Science*, 59(2), 327-338. <https://doi.org/10.1111/j.1365-2389.2007.01000x>

Keuper, F., van Bodegom, P. M., Dorrepaal, E., Weedon, J. T., van Hal, J., van Logtestijn, R. S. P., & Aerts, R. (2012). A frozen feast: Thawing permafrost increases plant-available nitrogen in subarctic peatlands. *Global Change Biology*, 18(6), 1998-2007. <https://doi.org/10.1111/j.1365-2486.2012.02663.x>

King, J. Y., Reeburgh, W. S., & Regli, S. K. (1998). Methane emission and transport by arctic sedges in Alaska: Results of a vegetation removal experiment. *Journal of Geophysical Research*, 103(D22), 29,083-29,092. <https://doi.org/10.1029/98JD00052>

Klapstein, S. J., Turetsky, M. R., McGuire, A. D., Harden, J. W., Czimczik, C. I., Xu, X., et al. (2014). Controls on methane released through ebullition in peatlands affected by permafrost degradation: Ebullition in peatlands with thermokarst. *Journal of Geophysical Research: Biogeosciences*, 119, 418-431. <https://doi.org/10.1002/2013JG002441>

Kokelj, S. V., & Jorgenson, M. T. (2013). Advances in thermokarst research. *Permafrost and Periglacial Processes*, 24(2), 108-119. <https://doi.org/10.1002/ppp.1779>

Kurylyk, B. L., MacQuarrie, K. T. B., & McKenzie, J. M. (2014). Climate change impacts on groundwater and soil temperatures in cold and temperate regions: Implications, mathematical theory, and emerging simulation tools. *Earth-Science Reviews*, 138, 313-334. <https://doi.org/10.1016/j.earscirev.2014.06.006>

Manies, K. L., Fjäller, C. C., Jones, M. C., Waldrop, M. P., & McGeehin, J. P. (2017). *Soil data for a thermokarst bog and the surrounding permafrost plateau forests located at Bonanza Creek Long Term Ecological Research Site, Interior Alaska* (USGS Numbered Series No. 2016-1173 (p.16)). Reston, VA: US Geological Survey. Retrieved from <http://pubs.er.usgs.gov/publication/ofr20161173>

McClain, M. E., Boyer, E. W., Dent, C. L., Gergel, S. E., Grimm, N. B., Groffman, P. M., et al. (2003). Biogeochemical hot spots and hot moments at the interface of terrestrial and aquatic ecosystems. *Ecosystems*, 6(4), 301-312. <https://doi.org/10.1007/s10021-003-0161-9>

Neumann, R. B., Blawie, S. J., Conaway, C. H., Turetsky, M. R., & Waldrop, M. P. (2016). Modeling CH<sub>4</sub> and CO<sub>2</sub> cycling using pore-water stable isotopes in a thermokarst bog in interior Alaska: Results from three conceptual reaction networks. *Biogeochemistry*, 127(1), 57-87. <https://doi.org/10.1007/s10533-015-0168-2>

NOAA. (2017). AgACIS for Fairbanks North Star Borough. Retrieved November 29, 2017, from <http://agacis.rcc-acis.org/?fips=02090>

Olefeldt, D., Turetsky, M.R., Crill, P.M., & McGuire, A.D. (2013). Environmental and physical controls on northern terrestrial methane emissions across permafrost zones. *Global Change Biology*, 19(2), 583. <https://doi.org/10.1111/gcb.12071>

Olivas, P. C., Oberbauer, S. F., Tweedie, C., Oechel, W. C., Lin, D., & Kuchy, A. (2011). Effects of fine-scale topography on CO<sub>2</sub> flux components of Alaskan coastal plain tundra: Response to contrasting growing seasons. *Arctic, Antarctic, and Alpine Research*, 43(2), 256-266. <https://doi.org/10.1657/1938-4246-43.2.256>

Poulter, B., Bousquet, P., Canadell, J.G., Ciais, P., Peregon, A., Saunois, M., et al. (2017). Global wetland contribution to 2000-2012 atmospheric methane growth rate dynamics. *Environmental Research Letters*, 12(9), 094013. <https://doi.org/10.1088/1748-9326/aa8391>

Quinton, W. L., Hayashi, M., & Chasmer, L. E. (2009). Peatland hydrology of discontinuous permafrost in the Northwest Territories: Overview and synthesis. *Canadian Water Resources Journal*, 34(4), 311-328. <http://doi.org/10.4295/cwrj3404311>

Reeve, A. S., Siegel, D. I., & Glaser, P. H. (2000). Simulating vertical flow in large peatlands. *Journal of Hydrology*, 227(1-4), 207-217. [https://doi.org/10.1016/S0022-1694\(99\)00183-3](https://doi.org/10.1016/S0022-1694(99)00183-3)

Saunois, M., Jackson, R. B., Bousquet, P., Poulter, B., & Canadell, J. G. (2016). The growing role of methane in anthropogenic climate change. *Environmental Research Letters*, 11(12), 120207. <https://doi.org/10.1088/1748-9326/11/12/120207>

Shaver, G.R., Johnson, L. C., Cades, D.H., Murray, G., Laundre, J.A., Rastetter, E.B., et al. (1998). Biomass and CO<sub>2</sub> flux in wet sedge tundras: Responses to nutrients, temperature, and light. *Ecological Monographs*, 68(1), 75-97. [http://doi.org/10.1890/0012-9518\(1998\)068\[0075:BACFIW\]2.0.C0:2](http://doi.org/10.1890/0012-9518(1998)068[0075:BACFIW]2.0.C0:2)

Turetsky, M.R., Kotowska, A., Bubier, J., Dise, N.B., Crill, P., Hombrook, E.R.C., et al. (2014). A synthesis of methane emissions from northern, temperate, and subtropical wetlands. *Global Change Biology*, 20(7), 2183-2197. <https://doi.org/10.1111/gcb.12580>

Turetsky, M. R., Treat, C. C., Waldrop, M. P., Waddington, J. M., Harden, J. W., & McGuire, A. D. (2008). Short-term response of methane fluxes and methanogen activity to water table and soil warming manipulations in an Alaskan peatland. *Journal of Geophysical Research*, 113, G00A10. <https://doi.org/10.1029/2007JG000496>

Turetsky, M.R., Wieder, R. K., & Vitt, D.H. (2002). Boreal peatland C fluxes under varying permafrost regimes. *Soil Biology and Biochemistry*, 34(7), 907-912. [https://doi.org/10.1016/S0038-0717\(02\)00022-6](https://doi.org/10.1016/S0038-0717(02)00022-6)

Turetsky, M. R., Wieder, R. K., Vitt, D. H., Evans, R. J., & Scott, K. D. (2007). The disappearance of relict permafrost in boreal North America: Effects on peatland carbon storage and fluxes. *Global Change Biology*, 13(9), 1922-1934. <https://doi.org/10.1111/j.1365-2486.2007.01381x>

van der Wal, R., & Stien, A. (2014). High-arctic plants like it hot: A long-term investigation of between-year variability in plant biomass. *Ecology*, 95(12), 3414-3427. <https://doi.org/10.1890/14-0533.1>

Waddington, J.M., & Rouleau, N. T. (1997). Groundwater flow and dissolved carbon movement in a boreal peatland. *Journal of Hydrology*, 191(1-4), 122-138. [https://doi.org/10.1016/S0022-1694\(96\)03075-2](https://doi.org/10.1016/S0022-1694(96)03075-2)

Walker, M.D., Wahren, C.H., Hollister, R.D., Henry, G.H. R., Ahlquist, L. E., Alatalo, J.M., et al. (2006). Plant community responses to experimental warming across the tundra biome. *Proceedings of the National Academy of Sciences*, 103(5), 1342-1346. <http://doi.org/10.1073/pnas.0503198103>

Yvon-Durocher, G., Allen, A. P., Bastviken, D., Conrad, R., Gudasz, C., St-Pierre, A., et al. (2014). Methane fluxes show consistent temperature dependence across microbial to ecosystem scales. *Nature*, 507(7493), 488-491. <https://doi.org/10.1038/nature13164>

Zhang, Z., Zimmermann, N.E., Stenke, A., Li, X., Hodson, E.L., Zhu, G., et al. (2017). Emerging role of wetland methane emissions in driving 21st century climate change. *Proceedings of the National Academy of Sciences*, 114(36), 9647-9652. <https://doi.org/10.1073/pnas.1618765114>